A. JABBAR HASSAN[1*], T. BOUKHAROUBA[1], D. MIROUD[2]

EFFECT OF FORGE APPLICATION ON MICROSTRUCTURAL AND MECHANICAL PROPERTIES OF AISI 316 USING DIRECT DRIVE FRICTION WELDING PROCESS

Present study introduces effect of forge application and elimination on microstructural and mechanical properties of AISI 316 during friction welding. Temperature measurements, microstructure, micro-hardness, tensile test, scanning electron microscopy and X-ray diffraction were evaluated. Maximum temperature recorded was 819°C while forge was applied between 357°C-237°C. Thermo-mechanically affected zone and highly plastically deformed zone were created at the interface at elimination and application of forge respectively. Ultimate tensile strength decreased and ductility increased when forge elimination compared to forge application. Tensile fracture was occurred adjacent to the welding interface for both cases, though, after forge application, ductile fracture mode and cleavage features through the fingerprints were observed in the fracture morphology. Redistribution and concentration of gamma iron in 111 level after forge application and heat treated of AISI 316.

Keywords: Friction welding; Forge phase; Micro-hardness; Ultimate tensile strength; X-ray diffraction

1. Introduction

Friction welding is a part of solid state welding process which produces joint below melting temperature of the metal being welded. It was used in several mechanical parts, such as, drive shafts, engine valves, pumps and compressor [1]. This process has several advantages: short time, low input energy, below melting temperature and high reproducibility [2-3]. Principally, it consists many processes: inertia [4], orbital [5], linear [6], friction stir [7-8] and direct drive friction welding (DDFW) [9].

In application, friction stir and DDFW are the most versatile. Friction stir creates soften metal at the welding area via pressure rotating pin tool against the base metal being welded [10]. While, DDFW generates heat by increasing temperature of the interface between the two pieces in contact under influence of axial pressure and rotation speed, first piece held in the stationary part and second piece chucked in the rotating part. The two pieces still in contact of each other until the rotation stops suddenly, this period is called friction phase, followed by pressure elevation for certain of time to consolidate welding joint and finish the process, this interval of time is known as forge phase [9].

Friction time, friction pessure, forge time, forge pressure and rotation speed are the principle conditions of DDFW. Bouarroudj et al. [1] and Titouche et al. [11] have exposed that with longer friction time, residual stresses and hard intermetallic compounds were created, which lead to reduce joint strength. Li et al. [12] have welded AA6061-T6 aluminum alloy by DDFW with different rotation speeds. Their results revealed the curves of friction time and friction work v.s. rotation speed, minimizing the values at 900 rpm. Although, Ajith et al. [13] have explained at high friction pressure, the values of hardness increase at the welding interface due to dynamic recrystallization, which causes grain refinement. Hazra et al. [14] have performed DDFW for high nitrogen steels and concluded reducing in tensile and impact strength relative to the base metal with elevation of forge force.

The concept used in the present has little attention in the literature survey, DDFW for AISI 316 by forge elimination in the first case and forge application in the second. Therefore, this study gives better and good idea about effect of forge on microstructural and mechanical properties of friction welding joint.

[1] HOUARI BOUMEDIENE UNIVERSITY OF SCIENCES AND TECHNOLOGY (USTHB), ADVANCED MECHANIC LABORATORY (LMA), BP. 32, EL-ALIA, 16111 BAB-EZZOAUR, ALGIERS-ALGERIA
[2] HOUARI BOUMEDIENE UNIVERSITY OF SCIENCES AND TECHNOLOGY (USTHB), MATERIALS SCIENCE AND PROCESS ENGINEERING LABORATORY (LSGM), BP. 32, EL-ALIA, 16111 BAB-EZZOAUR, ALGIERS-ALGERIA

* Corresponding author: jabbarhassan1973@yahoo.fr, (ammarjabbarhassan@gmail.com)

2. Material and methods

The commercial austenitic stainless used in current study has a symbol of AISI 316 according to American Institute for Steel and Iron with Ref. No. 440. The steel received as a long shaft with 6 m length and cut into small pieces for 45 mm length and 12 mm diameter. Microstructural and mechanical tests of this type of steel were performed in LMA and LSGM, USTHB, Algeria. This steel is highly content of Cr-Ni-Mo as demonstrated in TABLE 1 and excellent mechanical properties as revealed in TABLE 2. AISI 316 from the same group of AISI 304 but with high Molybdenum addition (Mo 2.93%). Mo improves resistance to non-oxidizing acides and pitting corrosion. Microstructure of AISI 316 in Fig. 1 shows difference austenitic equiaxed grains size.

TABLE 1

Alloying elements of AISI 316 (spectrum, wt. %)

C	Mn	Si	P	S	Mo	Cr	Ni
0.070	1.500	0.670	0.030	0.021	2.93	17.93	9.95

TABLE 2

Mechanical properties of AISI 316 (as it is)

UTS (MPa)	Young's modulus (MPa)	Elongation (%)	Average micro-hardness ($Hv_{0.1}$)
678-680	1.93×10^5	≈45	260-265

TABLE 3

Friction welding conditions

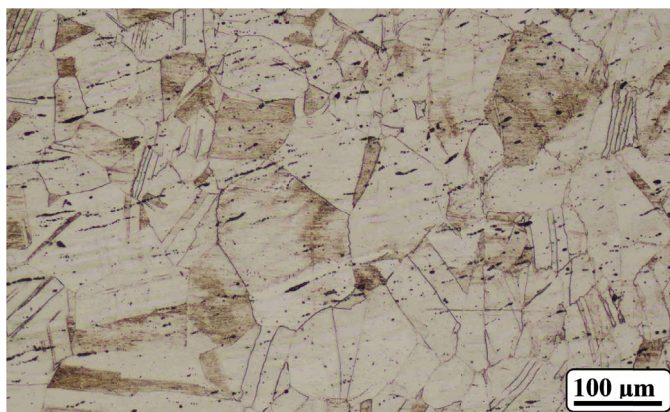| Rotation speed (r.p.m)	Friction pressure (MPa)	Friction time (s)	Forge pressure (MPa)	Forge time (s)
3000	130	10	—	—
3000	130	10	260	5

Fig. 1. Microstructure observation of AISI 316 [3]

DDFW machine used in this study was designed and fabricated in LMA, USTHB, Algeria as shown in Fig. 2. It has 3 phases AC with 3.5 kw power of motor, 0-3000 rpm range of speed and 300 MPa maximum pressure. Chosen friction welding conditions gathered in TABLE 3, the conditions were
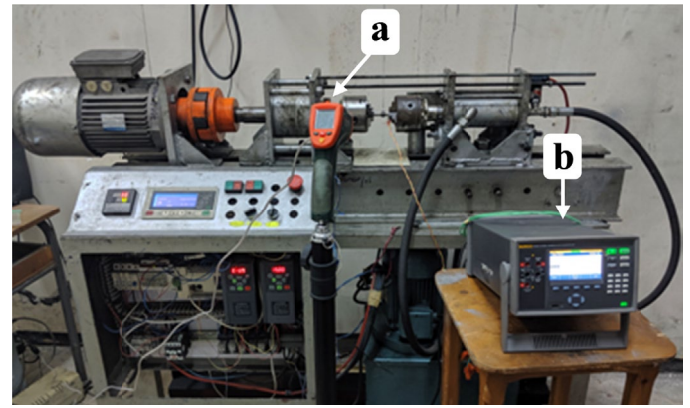

Fig. 2. Friction welding machine, (a) infrared thermometer, (b) thermometer by touch

selected according to the dimensions of test piece, metal nature and depending on the earlier studies [1,3,9,11,15]. Welding temperature was verified in two types of thermometer (Fig. 2), first thermometer by touch from type K, 0.5 mm wire diameter and maximum temperature is 1400°C with error ratio of ±50°C, the temperature tested closer to the center of the interface at the stationary part. Second thermometer by infrared from type K and maximum temperature is 1350°C with error ratio of ±50°C.

Macroscopic observations were carried out by NIKON SMZ 745T device to verify flash formation and determine location of tensile fracture with magnification of X 0.67. Microstructure observations were achieved by NIKON ECLIPSE LV100ND apparatus with magnification of X 100, while test pieces cut using a Presi mecatome T180 cutting machine. The test pieces embedded in a cold curing epoxy resin and polished with wet SiC abrasive paper up to 1200 grit and followed by polishing with 1 μm diamond polishing paste. The electrolyte etched for the test pieces was carried out by STRUERS LECTROPOL-5 equipment by 10 g oxalic acid hydrate and 90 ml water at 15 V for period of 300 s.

Scanning electron microscopy (SEM) was used for tensile fracture surface examination for forge case and AISI 316. The tests were realized by using JEOL JSM-6360 device with magnification of X 100. X-ray diffraction (XRD) was achieved by X'Pert PRO PANalytical for forge case, AISI 316 and by heat treatment of AISI 316 (819°C, soaking time for ½ h and air cooling), that permit to discover thermal effect alone and compares to thermo-mechanical influence of welding joint.

SHIMADZU HMV tester machine was utilized for microhardness measurements at room temperature condition, and according to ASTM E384 with used 100 gf indentation force and 10 s dwell time. The test pieces were cut by using a Presi mecatome T180 cutting machine, then the surfaces polished up to 1200 grit by wet SiC abrasive paper, followed by polishing on light disc cloth with 1 μm diamond paste and degreased with ethanol, and deionized water cleaning. Micro-hardness measurements were performed along the axial direction for welding joint.

Tensile tests were realized by INSTRON 5500 universal test machine with load capacity of ±100 kN. The quasi-static strain rate is 0.0016 s^{-1}. Tensile tests were carried out for all welding

joints as well as for AISI 316. The test pieces were cut by the lathe machine in the axial direction for standard specification of ISO 6892-1: 2009 (F). The effective diameter of tensile test piece is 6 mm as shown in Fig. 3. The welding line placed in the center of the specimen to obtain precise strain sensor position.
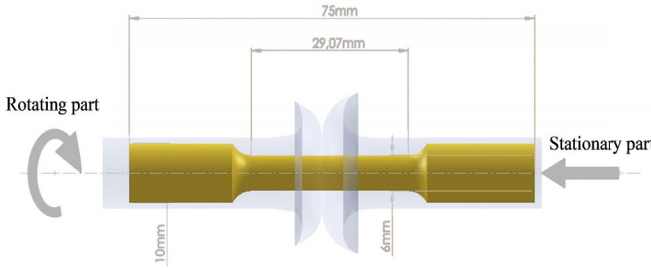

Fig. 3. Tensile test piece and its location in the welding piece

3. Results and discussion

Primarily, when the two parts are brought into contact under influence of rotation speed and friction pressure the friction is low and no increases in the temperature. Once the time passed 3.5 s the temperature rises rapidly and starts to create heat. The maximum temperature as illustrated in Fig. 4 remains localized at the interface of the two surfaces, which lead to plasticized the metal. Always under effect of rotation and friction pressure, during the remaining time of friction phase, part of the accumulated heat begins to diffuse until the friction time is terminated. That causes the soft metal at the interface to displace toward of the peripheral to form flash metal. The rotation stops suddenly and a forge pressure is applied under effect of forge temperature. Maximum temperature arrives to 819°C and forge applies between 357°C-237°C, that will influence on microstructure and mechanical properties of post-welding joint.

Therefore, as the temperature increases the accumulated heat causes the metal to be soften at the interfacial, under effect of rotation speed and axial pressure, the metal transfer toward the peripheral to form flash. Fig. 5 clarifies large amount of flash formation creation with forge application compared to forge elimination case, that could be explained by addition of forge phase and with remain applied of axial pressure and
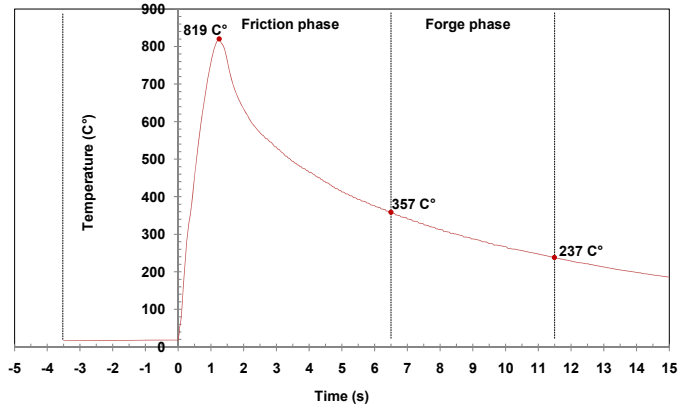

Fig. 4. Thermal curve introducing the average values of temperatures versus time during friction welding phases

temperature, the welding metal still soft and which will lead to large amount of flash formation. The amount of flash formation depends mainly on the mecahical properties of the welding metal [16]. In addition, the most important factors that effect on the degree of flash formation are thermo-plastic deformation [3], hardness and alloying elements [17]. The alloying elements Cr, Ni and Mo are responsible on refractory property of this type of stainless steel, which requests more force and temperature to obtain significant amount of flash formation.
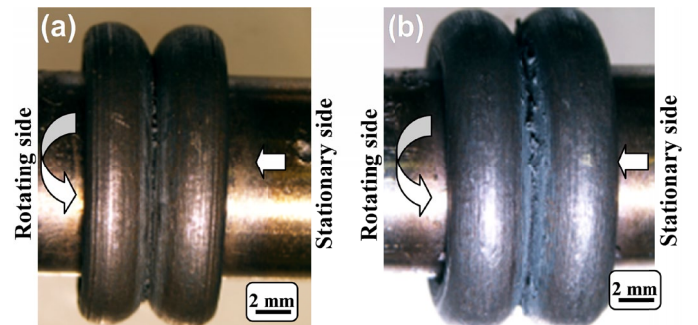

Fig. 5. Evolution of flash formation, (a) forge elimination, (b) forge application

Figs. 6(a) and (b) show microstructural investigation at elimination and application of forge respectively. Fig. 6(a)
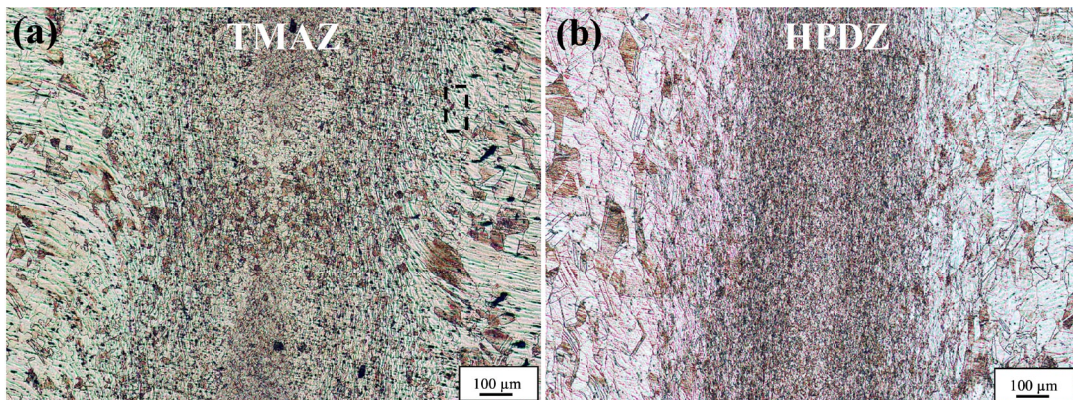

Fig. 6. Microstructure of welding center: (a) forge elimination, (b) forge application

demonstrates thermo-mechanically affected zone (TMAZ) at the interface of welding joint. This microstructure explains the influence during friction period under effect of axial pressure and rotation speed. Additionally, this zone is created because of period of friction which causes large amount of plastic deformation. However, under forge application (Fig. 6(b)) can distingue highly plastically deformation zone (HPDZ) at the interface, with very fine grains structure and moderately blackish color. After forge application and under effect of heat input and the rotation stopped, HPDZ created.

During forge phase, high plastic deformation and elevated temperature cause fine recrystallized grains forms, this phenomenon is called dynamic recrystallization. In addition, dynamic recrystallization depends on grain size, deformation conditions, chemical composition and nature of crystal structure [18]. HPDZ is easy to distinguish because that region is not etched at all cause of existence of very fine grains as a result of dynamic recrystallization [14]. On the other hand, the amount of heat input in the axial direction allows to expand of TMAZ due to cooling speed which lead to form of coarse grains [16].

Fig. 7 reveals micro-hardness profiles along the axial direction at forge elimination, which confirms general softening along the axial direction, this is due to formation of TMAZ during period of friction phase. Conversely, after forge application, the value of micro-hardness increases at the center of welding, as mentioned in the microstructural study, the thermo-plastic deformation and dynamic recrystallization responsible on grain refinement in the interface. Strain hardening [9] and high friction pressure [13] are most important conditions influence on the elevation of the micro-hardness, particularly, at the welding interface. While, micro-hardness attenuation in the adjacent regions after forge is due to enough amount of heat input which causes grains growth.

Fig. 8 exposes tensile test results at forge elimination and application as well as AISI 316. It shows ultimate tensile strength (UTS) decreased and ductility increased at forge elimination compared to forge application. Forge elimination illustrates reducing in UTS to 638 MPa and increasing in ductility to 0.371, that due to existence of soft structure (TMAZ) during friction phase cause of heat diffusion.

On the other hand, forge application case records high value of UTS closer to AISI 316 reaches to 670 MPa and reduces of
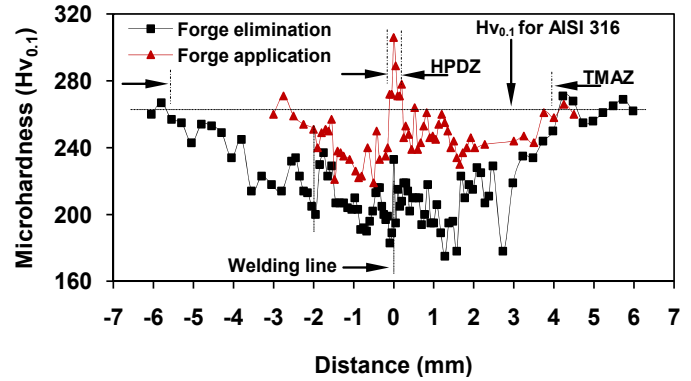

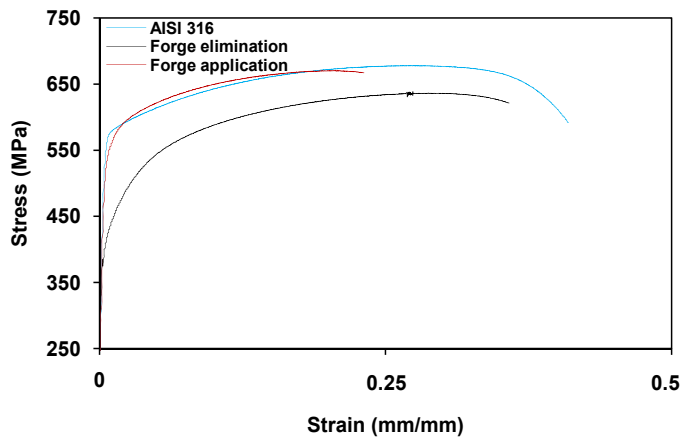Fig. 7. Micro-hardness profile along axial direction at forge elimination and application

Fig. 8. Tensile test curves at forge elimination and application with regard to AISI 316

ductility to 0.231. That because of high plastic deformation after forge application which lead to high level of micro-hardness due to HPDZ creation at welding center. Hazra et al. [14] have proved that the forge application is responsible on the increasing of micro-hardness at the interface and on reducing of UTS. Noticed, friction time as short as possible [19] while rotation speed, friction and forge pressure as high as possible [20], this leads to obtain high level of UTS.

The position of fracture as shown in Fig. 9 expose that the tensile fracture at forge elimination and application are
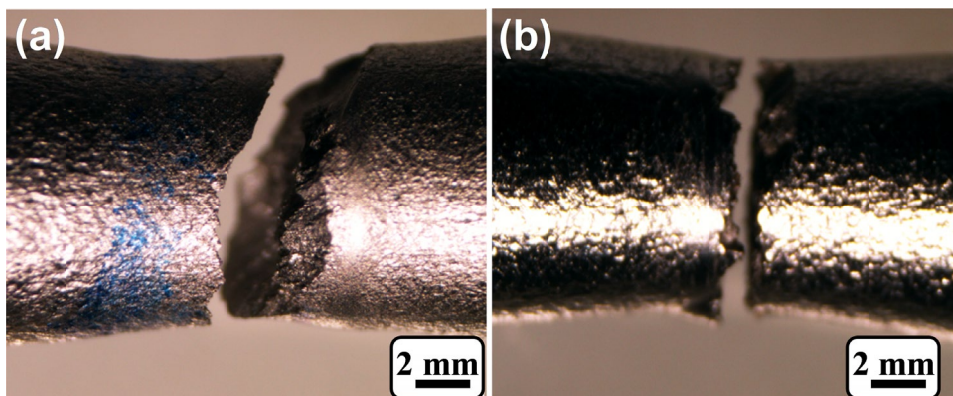

Fig. 9. Fracture nature of tensile test pieces: (a) forge elimination, (b) forge application
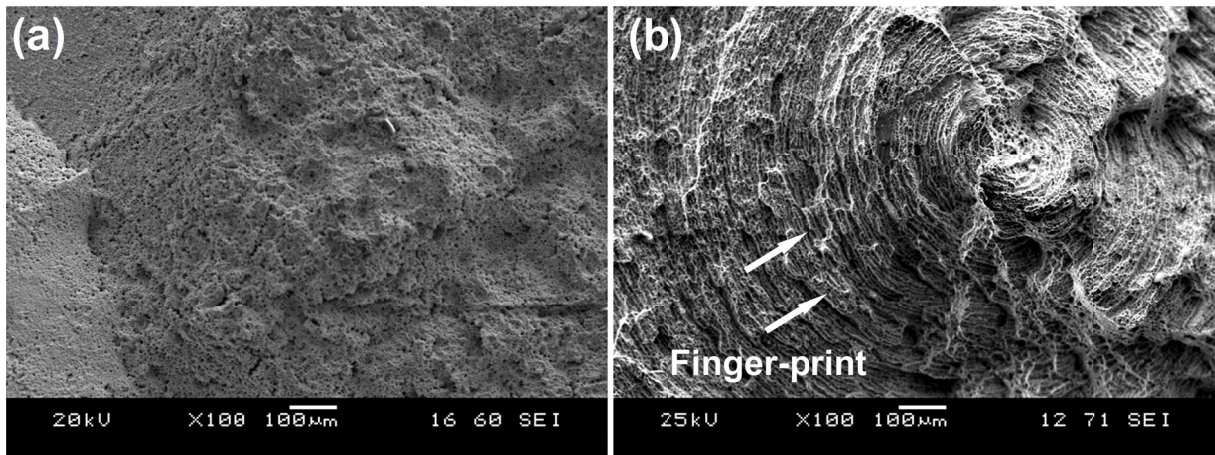
Fig. 10. SEM observation for forge application with regard to AISI 316: (a) AISI 316, (b) forge application
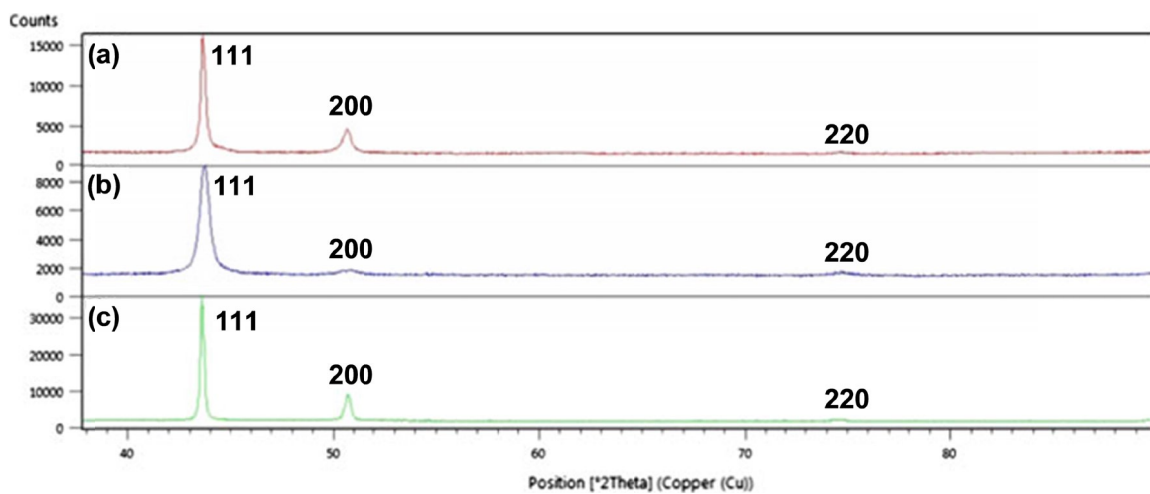

Fig. 11. XRD peaks: a) heat treated AISI 316, b) forge application, c) AISI 316 as it is

in the adjacent region of the welding interface. The reason of fracture position at neighboring is due to high amount of heat input absorbed, which cause a grain growth and responsible on weak in tensile strength. Thus, can be seen a reduction in cross sectional area placed at fracture position, this is a good sign of ductility behaviour.

The nature of fracture morphology by SEM for AISI 316 and forge case in Fig. 10(a) and (b) respectively, it reveals clear form of finger-print and can be seen a ductile fracture mode with cleavage features through the fingerprints, the last creates due to amount of thermo-plastic deformation under influence of high pressure and rotation speed [21], which lead the soft metal to flow from the center of the piece towards the peripheral during friction phase [22]. In addition, it seems also different forms of dimples with small cavities accumulate at the fracture position.

XRD analysis in Fig. 11 reveals redistribution and concentration of gamma iron in 111 level for both heat treated and forge case. Thus, XRD shows fine grains for the forge case and relatively fine grains for the heat treated case compared to AISI 316. That confirms of HPDZ creation and increases of micro-hradness at welding joint in the forge case.

4. Conclusions

Present work analyzed the effect of forge elimination and application during DDFW, the results summarized as following:

- Maximum temperature is 819°C and forge applies between 357°C-237°C,
- Forge elimination causes reducing amount of flash formation,
- Enlarge of TMAZ at forge elimination, and HPDZ under forge application,
- General softening along the axial direction created at forge elimination, while micro-hardness increases especially at the center of welding at forge application,
- Tensile tests results illustrate decreasing of UTS and increasing of ductility at forge elimination compared to forge application case,
- Tensile fractures for two cases take place neighboring to the interface,
- Ductile fracture mode with cleavage features and different form of dimples with small cavities accumulate at the tensile fracture position at forge application,

- XRD analysis reveals redistribution and concentration of gamma iron in 111 level for both heat treated and forge case, also fine grains for the forge case and relatively fine grains for the heat treated case compared to AISI 316.

REFERENCES

[1] E. Bouarroudj, S. Chikh, S. Abdi, D. Miroud, App. Therm. Eng. **110**, 1543-1553 (2017).

[2] C.H. Muralimohan, V. Muthupandi, K. Sivaprasad, Procedia Material Science **5**, 1120-1129 (2014).

[3] A.J. Hassan, T. Boukharouba, D. Miroud, S. Ramtani, Int. J. Eng. Transactions B: Applications **32** (2), 284-291 (2019).

[4] D.W. Mahaffey, O.N. Senkov, R. Shivpuri, S.L. Semiatin, Metall. Mater. Transactions A **47A**, 3981-4000 (2016).

[5] U. Raab, S. Levin, L. Wagner, C. Heinze, J. Mater. Process Technol. **215**, 189-192 (2015).

[6] P.S. Effertz, F. Fuchs, N. Enzinger, Int. J. Adv. Manuf. Technol. **92** (5-8), 2479-2486 (2017).

[7] P. Myśliwiec, R.E. Śliwa, R. Ostrowski, Arch. Metall. Mater. **64** (4), 1385-1394 (2019).

[8] T. Velmurugan, R. Subramanian, G. Suganya Priyadharshini, R. Raghu, Arch. Metall. Mater. **65** (2), 565-574 (2020).

[9] A.J. Hassan, T. Boukharouba, D. Miroud, Acta Metall. Slovaca **26** (3), 78-84 (2020),

[10] K.J. Quintana, J.L. Lopes Silveira, J. Manuf. Sci. and Eng. **139** (4), 041017-1-041017-8 (2017).

[11] N. Titouche, T. Boukharouba, S. Amzert, A.J. Hassan, R. Lechelah, S. Ramtani, J. Manuf. Processes **41**, 273-283 (2019).

[12] X. Li, J. Li, F. Jin, Weld World **62**, 923-930 (2018).

[13] P.M. Ajith, T.M. Afsal Husain, P. Sathiya, S. Aravindan, J. Iron Steel Res. Int. **22** (10), 954-960 (2015).

[14] M. Hazra, K.S. Rao, G.M. Reddy, J. Mater. Res. Technol. **3** (1), 90-100 (2014).

[15] A. J. Hassan, T. Boukharouba, D. Miroud, China Welding **28** (1), 42-48 (2019).

[16] G.I. Khidhir, S A. Baban, J. Mater. Res. Technol. **8** (2), 1926-1932 (2019).

[17] I. Kirik, N. Ozdemir, Int. J. Mater Res. **104** (8), 769-775 (2013).

[18] F.C. Liu, T.W. Nelson, Mater. Charact. **140**, 39-44 (2018).

[19] P. Sathiya, S. Aravindan, A. NoorulHaq, Int. J. Mech. Mater. Des. **3**, 309-318 (2006).

[20] N. Ozdemir, Mater. Lett. **59**, 2504-2509 (2005).

[21] R.A. Bell, J.C. Lippold, D.R. Adolphson, Weld. J. 325s-332s (1984).

[22] J.C. Lippold, B.C. Odegard, Weld. J. **63** (1), 35s-38s (1984).